Effect of thermal noise on the phase locking of a Josephson fluxon oscillator

Niels Grønbech-Jensen*
Physics Laboratory I, The Technical University of Denmark, DK-2800 Lyngby, Denmark

Mario Salerno
Department of Theoretical Physics, University of Salerno, I-84100 Salerno, Italy

Mogens R. Samuelsen
Physics Laboratory I, The Technical University of Denmark, DK-2800 Lyngby, Denmark
(Received 8 July 1991; revised manuscript received 2 March 1992)

The influence of thermal noise on fluxon motion in a long Josephson junction is investigated when the motion is phase locked to an external microwave signal. It is demonstrated that the thermal noise can be treated theoretically within the context of a two-dimensional map that models the dynamics of a single fluxon.

I. INTRODUCTION

Phase-locking of fluxon motion to an external signal (electric or magnetic)[1] has been extensively investigated[2–5] using a simple particle model that captures many of the characteristics observed experimentally in long Josephson junctions (LJJ's). This simple semianalytical model reduces the perturbed sine-Gordon[6] (SG) equation to an implicit two-dimensional map under the following assumptions. The influence of the external ac drive on the system is felt only through the boundary conditions, and there is exactly *one* fluxon present in the junction at *all* times. In the special case where all input power acts only through the boundary conditions (the in-line junction), the two-dimensional map becomes explicit, and hence, it is possible to develop analytical expressions for the existence of fixpoints (phase-locked states) and their stability. When the fluxon is in a phase-locked state it has been observed[4] that the stability of the fixpoint changes as relevant system parameters are varied within the locking range. This can, under certain circumstances, result in period doubling bifurcations, which may lead to chaotic oscillations of the soliton propagation. It was shown that the instability of the fundamental mode (period one) appears near the center of the phase-locked step in the dc *I-V* curve of a LJJ.

The aim of the present paper is to investigate the effect of thermal noise on the phase-locked state, and hereby show that noise measurements can be used to detect internal bifurcations in the system. Our investigation is also relevant to the prediction of the linewidth of the emitted signal from a phase-locked LJJ since the linewidth increases with the variance of the time of flight for the fluxon.[7] The effect of noise on steady-state fluxon motion in an infinite-length LJJ has previously been considered in Refs. 7–9. We will study the problem from different levels of approximation and compare the results. Further, we present a simple way of implementing thermal noise into the map formalism. We show that this stochastic-map formalism agrees well with the more complete model of continuous time. Also, it is found that the measured noise level depends critically on the frequency at which the measurement is performed. This, together with other characteristics, indicates that the system enters a "squeezed state" when it is operated near instability points on phase-locked steps.

II. THEORY

It is assumed that the LJJ is well described by the perturbed SG equation given by[9]

$$\phi_{xx}-\phi_{tt}-\sin\phi=\alpha\phi_t-\beta\phi_{xxt}-\eta-n(x,t)\ , \tag{1}$$

where ϕ is the quantum phase difference between the superconductors of the junction and $n(x,t)$ is the stochastic force associated with the loss terms ($\sim\alpha$ and $\sim\beta$). In Ref. 9 it was shown that the autocorrelation of this stochastic process could be chosen to be

$$R_{nn}(x,x',t,t')=\langle n(x,t)n(x',t')\rangle = 16\frac{kT}{E_0}\delta(t-t')\left[\alpha-\beta\frac{\partial^2}{\partial x^2}\right]\delta(x-x')\ , \tag{2}$$

where k is the Boltzmann constant, T is the temperature, δ is the Dirac delta function, and E_0 is the soliton rest energy given by

$$E_0=8\frac{\hbar JW\lambda_J}{2e}\ , \tag{3}$$

where J is the critical current density, W is the width of the junction, λ_J is the Josephson penetration length, and Δ is the energy gap of the superconductor.

If we denote the junction length by L, we have the boundary conditions[10]

$$\begin{aligned}&\phi_x(0,t)+\beta\phi_{xt}(0,t)=\kappa_m(t)-\kappa_e(t)\ ,\\ &\phi_x(L,t)+\beta\phi_{xt}(L,t)=\kappa_m(t)+\kappa_e(t)\ ,\end{aligned} \tag{4}$$

where κ_m represents an external magnetic field and κ_e represents the in-line nature of the junction bias current.

Introducing the unperturbed kink profile, representing the fluxon in the junction, we have

$$\phi(x,t)=4\tan^{-1}[\gamma(u)(x-x_0)] , \tag{5}$$

where x_0 is the soliton position, u is the normalized velocity of the fluxon, and $\gamma(u)=1/\sqrt{1-u^2}$ is the inverse Lorentz contraction. Defining the wave momentum P of the system as

$$P(t)=-\frac{1}{8}\int \phi_x\phi_t dx , \tag{6}$$

we can immediately find the equation of motion for the reduced coordinates (x_0,P) of the fluxon in the interior of the junction:

$$\begin{aligned}\frac{dP}{dt}&=-\alpha P-\frac{1}{3}\beta P(1+P^2)+\frac{\pi\eta}{4}+\epsilon(t) ,\\ \frac{dx_0}{dt}&=\frac{P}{\sqrt{1+P^2}} ,\end{aligned} \tag{7}$$

where the soliton profile of Eq. (5) gives

$$P=\frac{u}{\sqrt{1-u^2}}, \quad u\equiv\frac{dx_0}{dt} . \tag{8}$$

The term $\epsilon(t)$ represents the projection of the stochastic force into the soliton profile. The autocorrelation of ϵ is easily found to be

$$R_{\epsilon\epsilon}(\tau)=2\frac{kT}{E_0}\gamma(u)\left[\alpha+\frac{1}{3}\beta\gamma^2(u)\right]\delta(\tau), \quad \tau=t-t' \tag{9}$$

i.e., an autocorrelation function representing white noise. Note that $\epsilon(t)$ is not in the general case a stationary process, since $u=\dot{x}_0$ is a function of time. Solving the equations of motion for (x_0,P) we need to consider the influence of the boundary reflections at $x_0=0$ and $x_0=L$. Following the treatment outlined in Refs. 2 and 3, we treat the reflection time as negligible compared to the period of any external signal (κ_m or κ_e). Hence, the energy contribution (input) to the fluxon motion during a reflection at the time $t=t_k$ is given by

$$\begin{aligned}\Delta H_k&=\frac{\pi}{2}[\kappa_e(t_k)-\kappa_m(t_k)], \quad \text{at } x_0=0\\ \Delta H_k&=\frac{\pi}{2}[\kappa_e(t_k)+\kappa_m(t_k)], \quad \text{at } x_0=L\end{aligned} \tag{10}$$

where the energy is normalized to E_0.

Other contributions affecting the boundary reflections are discussed in detail in Ref. 3, but these additional terms, describing increased loss and a phase shift during reflection, are not of our present interest and are neglected here. For oscillating external fields, κ_e and κ_m, the phase-locked states are created by an adjustment of the internal phase relation between the actual reflection times t_k and the oscillating field, in order to supply the fluxon with a sufficient energy shift [Eq. (10)], giving the required average velocity.

The original problem of solving a stochastic partial differential equation (PDE) has now been reduced to the problem of solving a stochastic second-order ordinary differential equation (ODE) Eq. (7) with the boundary conditions Eq. (10), given that the relation between the momentum and the energy is

$$uH=P . \tag{11}$$

Although this is a drastic reduction of the original problem [Eq. (1)], it is still much more time consuming to solve this equation than to obtain the solution of a two-dimensional map, in which the motion from $x_0=0$ to $x_0=L$ is evaluated in one iteration. The problem of reducing the Langevin equation Eq. (7) to a map lies in the stochastic term $\epsilon(t)$, which must be considered to be continuous in time. However, it turns out that an accumulated equivalent to the noise term $\epsilon(t)$ can be included in the map description in a simple manner, and hence, the problem can be reduced to a two-dimensional stochastic map.

Throughout this paper, we choose system parameters similar to the ones treated in Ref. 4. Hence, we consider the in-line junction case only, and set $\eta=0$. We now briefly sketch the derivation of the explicit map model that we will be concerned with here. We assume that $\eta=\beta=0$ in Eq. (7) and we initially neglect the stochastic term $\epsilon(t)$. Equation (7) can then be integrated twice to give

$$x_0(t)=x_0(t_k)+\frac{1}{\alpha}[\sinh^{-1}(P_k)-\sinh^{-1}(P_k e^{-\alpha(t-t_k)})] . \tag{12}$$

Here subscript k denotes that the quantity is evaluated at the time t_k, which is the time of the previous reflection at a boundary. Thus the time t is restricted to be in the interval $t\in[t_k,t_{k+1}]$ between two reflections. Inserting $t=t_{k+1}$ into Eq. (12), we find the time of flight for the soliton to traverse the junction length L:

$$t_{k+1}-t_k=\frac{1}{\alpha}\ln\left[\frac{\sinh a_k}{\sinh(a_k-\alpha L)}\right] , \tag{13}$$

where $a_k=\sinh^{-1}P_k$. At $t=t_{k+1}$ the soliton undergoes a reflection, causing an energy shift given by (no energy dissipation) Eqs. (10). Using the relation between the soliton energy and momentum Eq. (11) we obtain the following expression for the value of a_{k+1}:

$$\cosh(a_{k+1})=\cosh(a_k-\alpha L)+\Delta H , \tag{14}$$

where ΔH for an in-line junction in an external ac field with the frequency ω_{ac} is

$$\Delta H=(\pi/2)[\kappa_{dc}+\kappa_{ac}\sin(\omega_{ac}t_{k+1}+\theta)] , \tag{15}$$

where a phase angle is given by θ. The total normalized bias current forced through the junction is $2\kappa_{dc}$ and the accumulated normalized time is t_k. The amplitude κ_{ac} is in the electric coupling case a constant and in the magnetic coupling case it is given by $\kappa_{ac}=|\kappa_{ac}|(-1)^k$.

Introducing the time variable T_k and the energy variable U_k by

$$T_k = t_k \left[\mathrm{mod} \frac{2\pi}{\omega_{ac}} \right] ,$$
$$U_k = \cosh a_k , \tag{16}$$

we have the explicit two-dimensional map given by

$$T_{k+1} = T_k + \frac{1}{\alpha} \ln \left[\frac{\sqrt{U_k^2 - 1}}{C\sqrt{U_k^2 - 1} - SU_k} \right] \left[\mathrm{mod} \frac{2\pi}{\omega_{ac}} \right] ,$$
$$U_{k+1} = CU_k - S\sqrt{U_k^2 - 1} + \frac{\pi}{2}[\kappa_{dc} + \kappa_{ac} \sin(\omega_{ac} T_{k+1} + \theta)] , \tag{17}$$

where the constants S and C are $\sinh(\alpha L)$ and $\cosh(\alpha L)$, respectively. Looking for phase-locked states of the fluxon motion, when the junction is coupled to an ac signal, we will assume that the map Eq. (17) has fixpoints (T^*, U^*) given by the conditions $T_{k+1} = T_k$ and $U_{k+1} = U_k$. These period-one fixpoints were found[3,4] to be given by

$$T^* = \frac{1}{\omega_{ac}} \left[\sin^{-1} \left[\frac{\bar{K} - \kappa_{dc}}{\kappa_{ac}} \right] - \theta \right] ,$$
$$U^* = \frac{C - E}{\sqrt{(C-E)^2 - S^2}} , \tag{18}$$

where

$$E = \exp \left[-\frac{m\pi\alpha}{\omega_{ac}} \right] ,$$
$$\bar{K} = \frac{2(C-1)(1+E)}{\pi\sqrt{1 - 2EC + E^2}} . \tag{19}$$

Here the integer m denotes that the state under consideration is the mth subharmonic of the driving signal. Since the argument to the inverse sine function in Eq. (18) should be numerically less than one, the existence of the fixpoints (phase-locked states) requires that the following condition is fulfilled:

$$\bar{K} - \kappa_{ac} < \kappa_{dc} < \bar{K} + \kappa_{ac} . \tag{20}$$

Since our interest here is to investigate the effect of noise on a phase-locked step, we will now investigate how a small displacement $(\delta T, \delta U)$ from the fixpoint (T^*, U^*) affects the system. First we note, as was mentioned in Refs. 2–4, that for $\alpha > 0$, the phase space is always contracting between boundary reflections, since the Jacobian $\underline{J}$ of the map is given by[11]

$$|\det \underline{J}| = e^{-\alpha(T_{k+1} - T_k)} . \tag{21}$$

However, the linear stability analysis of the fixpoint in Eq. (18) shows[4] that the stability can break down near the center of the phase-locked step. Here analytical expressions for the two eigenvalues λ_i $(i = 1,2)$ of the Jacobian for the fixpoints of the diagonalized map are given:

$$\lambda_i = \frac{1 + E - A}{2} \pm \left[\left[\frac{1 + E - A}{2} \right]^2 - E \right]^{1/2} , \quad \lambda_1 \lambda_2 = E$$
$$A = \left[\frac{\tanh^2 \left[\frac{\alpha m \pi}{2\omega_{ac}} \right]}{\tanh^2 \left[\frac{\alpha L}{2} \right]} - 1 \right]^{3/2} \frac{\cosh^3 \left[\frac{\alpha m \pi}{2\omega_{ac}} \right]}{\cosh^3 \left[\frac{\alpha L}{2} \right]}$$
$$\times \sinh(\alpha L) \frac{\pi \omega_{ac} \kappa_{ac}}{2\alpha} E^{1/2} \cos\psi , \tag{22}$$

$$\sin\psi = \frac{1}{\kappa_{ac}} \left\{ 4\pi \frac{\sinh \left[\frac{\alpha L}{2} \right]}{\left[\frac{\tanh^2 \left[\frac{\alpha m \pi}{2\omega_{ac}} \right]}{\tanh^2 \left[\frac{\alpha L}{2} \right]} - 1 \right]^{1/2}} - \kappa_{dc} \right\} .$$

From this expression it is not immediately evident how the stability of the period-one phase-locked state behaves. However, in Fig. 1 we have plotted the eigenvalues as a function of the dc bias κ_{dc} for two different values of the ac bias amplitude. The system parameters are chosen to be like the ones used in Ref. 4: $\alpha = 0.05$, $L = 12$, $\omega_{ac} = 1.5$, and $m = 8$ for electric coupling of the ac field. In this case, we find that an instability $\lambda_i \approx 1$ coincides with the boundaries of the existence of the phase-locked state. This instability is not our main interest here, since it could be predicted from the much simpler analysis of the existence of the fixpoints. Further, these eigenvalues break up on the *positive* real axis, so that no period doubling bifurcation is possible. A more interesting situation is present near the center of the phase-locked step. As can be seen from Fig. 1, the two eigenvalues can—if the ac drive is strong enough—break up on the *negative* real axis in some interval of κ_{dc}. A significant difference between the two situations of $\kappa_{ac} = 0.16$ and $\kappa_{ac} = 0.18$ is that in the first case, none of the eigenvalues exceeds the unit circle in the negative direction of the real axis, whereas in the second case one of the eigenvalues exceeds -1 in the negative direction, causing a period doubling bifurcation in the motion of one of the dynamical variables of the diagonalized map, as also reported in Ref. 4.

To proceed in our analysis of the effect of noise, we need to reintroduce the stochastic term in the dynamical equations. In order to preserve the dynamical equations as a map, we must derive analytical equations for the accumulated noise contributions to the two dimensions—time and energy—for a fluxon traveling the distance L through the junction. Since the following treatment is based on the theory of stationary stochastic processes, it is only strictly valid if the fluxon velocity deviates only slightly from the average velocity. Therefore it is probably better for an overlap junction than for an in-line junction.

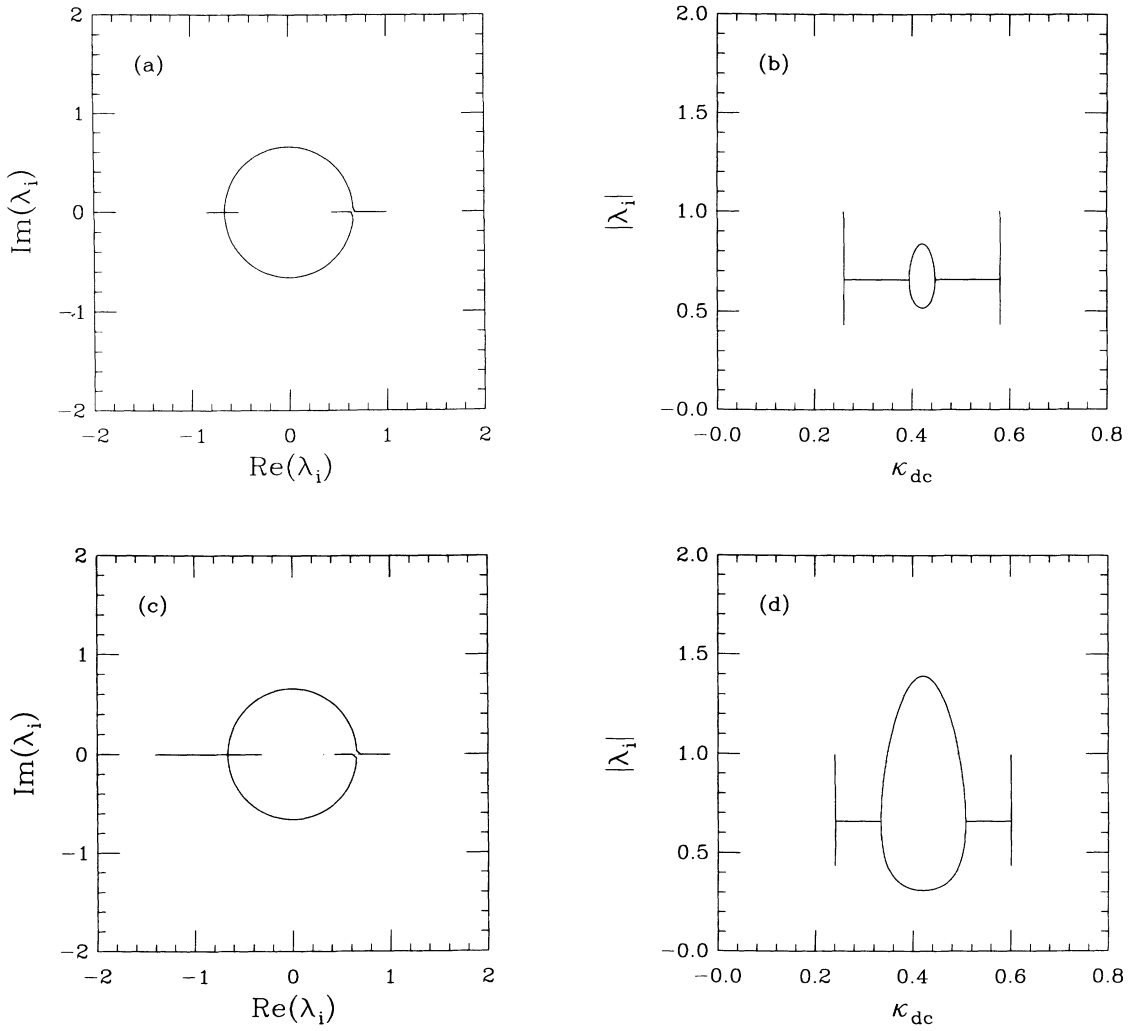

FIG. 1. The two eigenvalues of the phase-locked period-one state as a function of the dc bias current. The parameters are: $L=12$, $\alpha=0.05$, $\omega_{ac}=1.5$, and $m=8$. The dc bias κ_{dc} is varied through the locking range. (a) The imaginary parts of λ_i as a function of the real parts for the case of $\kappa_{ac}=0.16$. (b) The absolute values $|\lambda_i|$ as a function of κ_{dc} for the case of $\kappa_{ac}=0.16$. (c) The imaginary parts of λ_i as a function of the real parts for the case of $\kappa_{ac}=0.18$. (d) The absolute values $|\lambda_i|$ as a function of κ_{dc} for the case of $\kappa_{ac}=0.18$.

The time of flight is given by

$$T=\int_0^L \frac{1}{u}dx \ . \tag{23}$$

Since we treat the noise as a small-amplitude stochastic process, we write

$$T=T_0+\delta T \ , \tag{24}$$

where T_0 denotes the time of flight for the fluxon in a noiseless system and δT denotes the stochastic influence given by

$$\delta T\approx-\int_0^{T_0}\frac{\delta u}{u}dt\approx-\int_0^{T_0}\frac{\delta u}{\langle u\rangle}dt \ , \tag{25}$$

where we have assumed that we can consider the average velocity only. Assuming that all involved processes are stationary and normal with zero average, we have the variance of δT as[12]

$$\sigma^2_{\delta T\,\delta T}\approx\int_0^{T_0}\int_0^{T_0}\frac{R_{\delta u\,\delta u}(t_2-t_1)}{\langle u\rangle^2}dt_1dt_2$$
$$=\int_0^{T_0}\int_0^{T_0}\frac{1}{\langle u\rangle^2}\left\langle\frac{\partial u}{\partial P}\right\rangle^2 R_{\delta P\,\delta P}(t_2-t_1)dt_1dt_2 \ , \tag{26}$$

where the autocorrelation function $R_{\delta P\,\delta P}(t_2-t_1)$ for the momentum fluctuation is found from the linearized equation for the momentum noise:

$$\frac{d\delta P}{dt}=-\alpha\delta P-\tfrac{1}{3}\beta\delta P-\beta P_0^2\delta P+\epsilon(t) \ , \tag{27}$$

where $P_0(t)$ is the momentum of the system with no noise. Denoting the power spectrum by $S(\omega)$ we have

$$R_{\delta P\,\delta P}(\tau)=\frac{1}{2\pi}\int S_{\delta P\,\delta P}(\omega)e^{j\omega\tau}d\omega$$
$$=\frac{1}{2\pi}\int\frac{S_{\epsilon\epsilon}(\omega)}{(\alpha+\beta/3+\beta P_0^2)^2+\omega^2}e^{j\omega\tau}d\omega$$
$$=\frac{S_{\epsilon\epsilon}(0)}{4\pi(\alpha+\beta/3+\beta P_0^2)}e^{-(\alpha+\beta/3+\beta P_0^2)|\tau|}, \quad (28)$$

where the time variable $\tau=t_2-t_1$ is introduced for the stationary processes. Applying this expression in Eq. (26) we find the accumulated noise of the time of flight to be given by

$$\sigma^2_{\delta T\,\delta T}\approx\frac{kT}{E_0}\frac{1}{\pi}\frac{1}{u^2\gamma^5(u)}\frac{\alpha+\frac{1}{3}\beta(1+P^2)}{(\alpha+\frac{1}{3}\beta+\beta P^2)^2}$$
$$\times\left[T_0-\frac{1}{\alpha+\frac{1}{3}\beta+\beta P^2}(1-e^{-(\alpha+\beta/3+\beta P^2)T_0})\right], \quad (29)$$

where

$$u\approx\frac{L}{T_0},\quad P\approx\frac{L/T_0}{\sqrt{1-(L/T_0)^2}}. \quad (30)$$

Hence, a stochastic process with the variance given by Eq. (29) can be added to the map in the equation for the time of flight. Similarly the noise contribution to the dimension U can be considered to be a stochastic process with the variance given by

$$\sigma^2_{\delta U\,\delta U}\approx\left[\frac{\partial U}{\partial P}\right]^2 R_{\delta P\,\delta P}(0)$$
$$\approx\frac{kT}{E_0}\frac{1}{2\pi}\frac{\alpha+(\beta/3)(1+P^2)}{\alpha+\beta/3+\beta P^2}P. \quad (31)$$

In most cases the noise amplitude Eq. (29) of the time of flight is the dominant of the two contributions [Eqs. (29) and (31)], since this term is an accumulated quantity whereas the noise of the momentum in the map is dependent on the momentum at the reflection times alone. In the above treatment of the noise amplitudes, the correlation in time and the correlation between the two noise components have been neglected completely. However, as we will see, this does not seem to be important. Also the results do not depend critically on the actual distribution of the stochastic processes.

Finally, in this semianalytical treatment of the noise properties, let us make some simple predictions. For simplicity, we will only be concerned with the diagonalized map (two one-dimensional maps). Denoting the leading eigenvalue by λ_1 ($|\lambda_1|\geq|\lambda_2|$) and the corresponding variable (fixpoint) by X^*, we have the one-dimensional map

$$X_{k+1}=X^*+\lambda_1\xi_k+s_k \Longrightarrow \xi_{k+1}=\lambda_1\xi_k+s_k, \quad (32)$$

where ξ_k is a small displacement from the fixpoint and s_k is the projected noise contribution to the variable X. If we assume that s_k is uncorrelated in k and a stationary process, we immediately find the variance of ξ_k to be[13]

$$\langle\xi_k^2\rangle=\frac{\langle s_k^2\rangle}{1-\lambda_1^2}. \quad (33)$$

From this expression, it is evident that near an instability ($|\lambda_1|$ close to one) the noise in some direction in the two-dimensional phase space of the two-dimensional map increases. This will in general, of course, affect the two physical dimensions of time and momentum. Hence, we can expect to observe increased fluctuations in voltage measurements over the time of flight, as we approach the bifurcation points or—in the case of no bifurcations—as we approach the center of the phase-locked step. However, if we measure the voltage over two periods ($2T^*$), a completely different situation arises. Writing the sum of the displacements of two successive iterations, we have

$$\xi_k+\xi_{k+1}=(\lambda_1+1)\xi_k+s_k. \quad (34)$$

From this expression, we get the variance of the noise on a measurement of X made over two iterations:

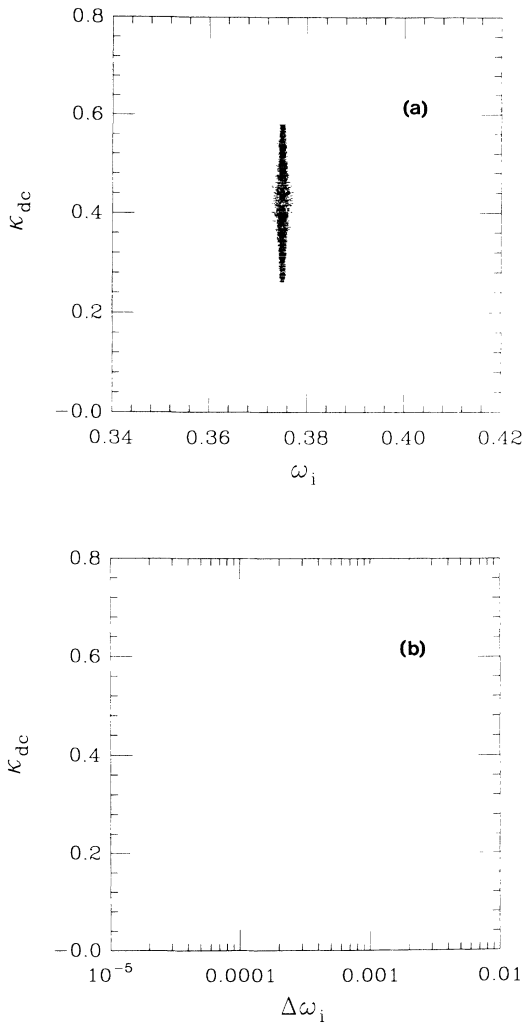

FIG. 2. Results of the stochastic ordinary differential equation [Eq. (7)] for the parameters of Fig. 1(a) and for a temperature of $kT/E_0=10^{-6}$. (a) Measurements of the frequencies $\omega_i=2\pi/T_i$. (b) The standard deviation $\Delta\omega_i$ of the measurements in (a).

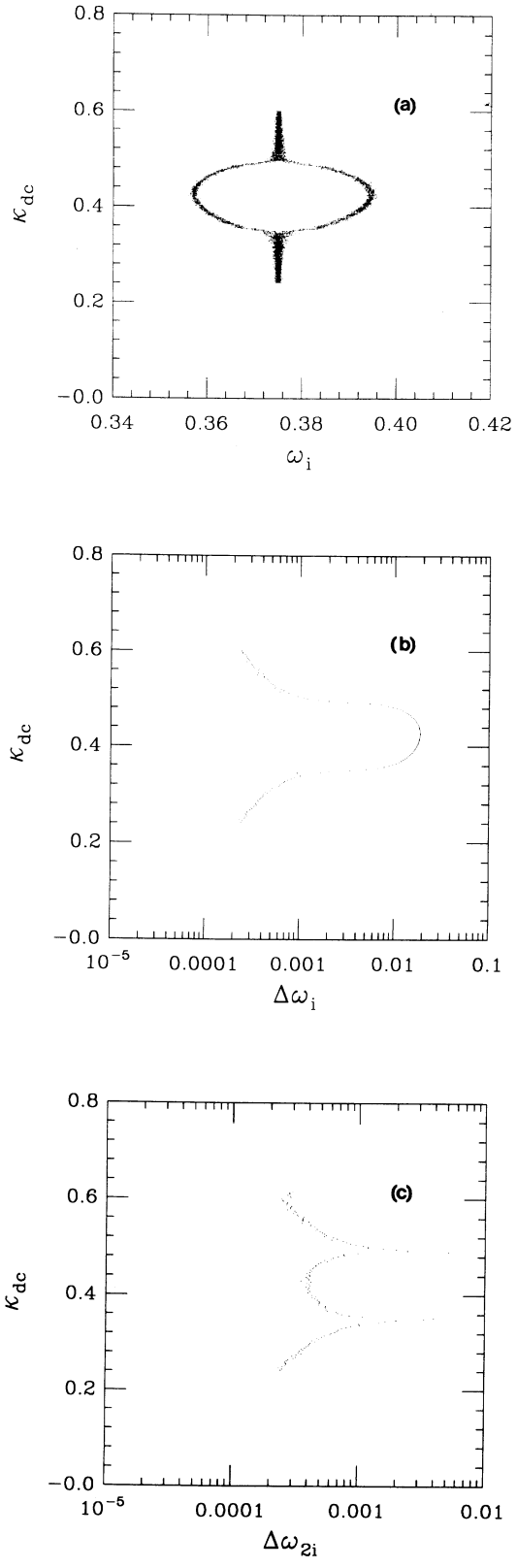

FIG. 3. Results of the stochastic ordinary differential equation [Eq. (7)] for the parameters of Fig. 1(c) and for a temperature of $kT/E_0=10^{-6}$. (a) Measurements of the frequencies $\omega_i=2\pi/T_i$. (b) The standard deviation $\Delta\omega_i$ of the measurements in (a). (c) The standard deviation $\Delta\omega_{2i}$ obtained from every second measurement of ω_i.

$$\langle(\xi_k+\xi_{k+1})^2\rangle=\frac{2}{1-\lambda_1}\langle s_k^2\rangle \ . \tag{35}$$

Since the instability points of interest are located on the negative real axis, the variance of Eq. (35) is a well behaved function of λ_1. In fact, the noise level of measurements made over two periods decreases as we approach the instability $\lambda_1\rightarrow -1$, which is exactly opposite the case of measurements made over one period of the motion [Eq. (33)].

III. NUMERICAL EXPERIMENTS

In order to observe some of the predicted features and to compare the results of the noise expressions developed for the map, we have made numerical experiments on the two models described above. The chosen parameters are

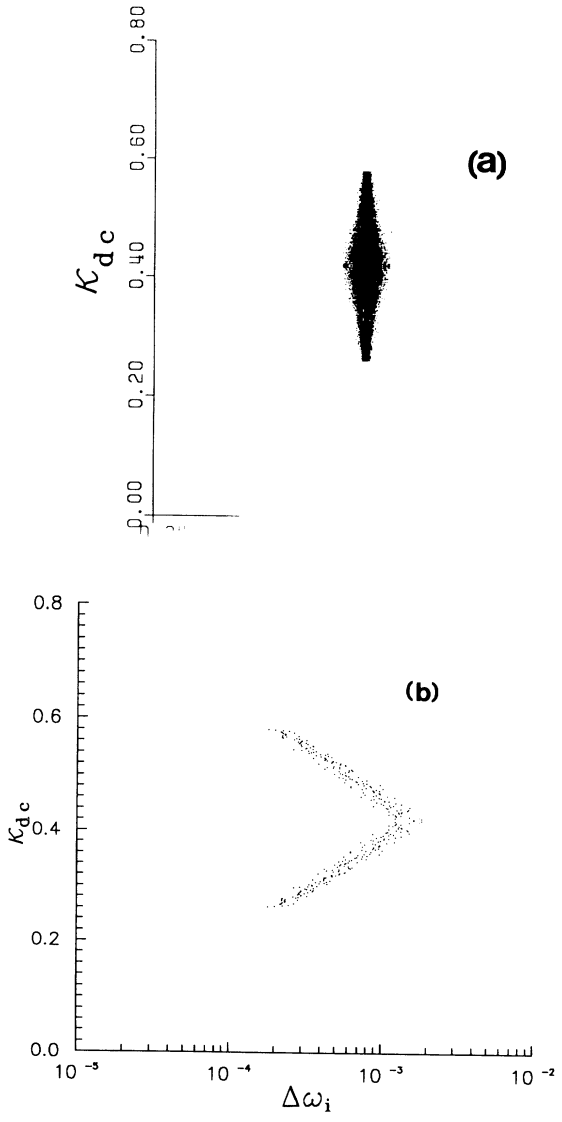

FIG. 4. Results of the stochastic map for the parameters of Fig. 1(a) and for Gaussian noise amplitudes of $\delta_T=0.01$ and $\delta_U=0$. (a) Measurements of the frequencies $\omega_i=2\pi/T_i$. (b) The standard deviation $\Delta\omega_i$ of the measurements in (a).

$L=12$, $\alpha=0.05$, $\beta=0$, $\kappa_m=0$ (electric coupling), $\eta=0$ (in-line junction), and $\omega_{ac}=1.5$ ($m=8$). Two characteristically different values of the ac bias current κ_{ac} have been chosen, one value which does not give rise to a bifurcation ($\kappa_{ac}=0.16$), and one ($\kappa_{ac}=0.18$) which does. In Figs. 2 and 3 we show the results of the ODE model of Eq. (7). Here we have solved the coupled stochastic differential equations by use of a second- (and third-) order Runge-Kutta-like method for stochastic differential equations.[14,15] The solution was obtained by following the trace x_0 in the interval $[0,L]$ and applying the boundary conditions of Eq. (10) [Eq. (15)]. A time step of $dt=0.01$ was found to be quite sufficient to describe the traveling soliton. The stochastic term in the equation was generated by a standard random number generator for uniformly distributed numbers followed by a transformation into a Gaussian distribution.[16] The variance was adjusted at all times in accordance with Eq. (9), and a normalized temperature of $kT/E_0=10^{-6}$ was chosen as an example. The system was allowed a transient time of 400 periods (times of flight through the junction). Figure 2(a) shows 100 measured frequencies $\omega_i=2\pi/T_i$ for each value of the normalized bias current κ_{dc} in the locking range. In this figure we find a vertical step in the dc I-V curve corresponding to phase locking, but we also find that the "noisy" ensemble of points has a larger deviation from the average near the center of the step—as predicted by Eq. (33). This is more evident when we look at Fig. 2(b), where we have calculated the standard deviation $\Delta\omega_i=\sqrt{\langle\omega_i^2\rangle-\langle\omega_i\rangle^2}$ of 1000 successive measurements of ω_i. The locking range is very clearly characterized by a large noise level near the center. Note that the noise level in this variable (T_k) increases from the edge of the step to the center of the step, whereas the analysis pre-

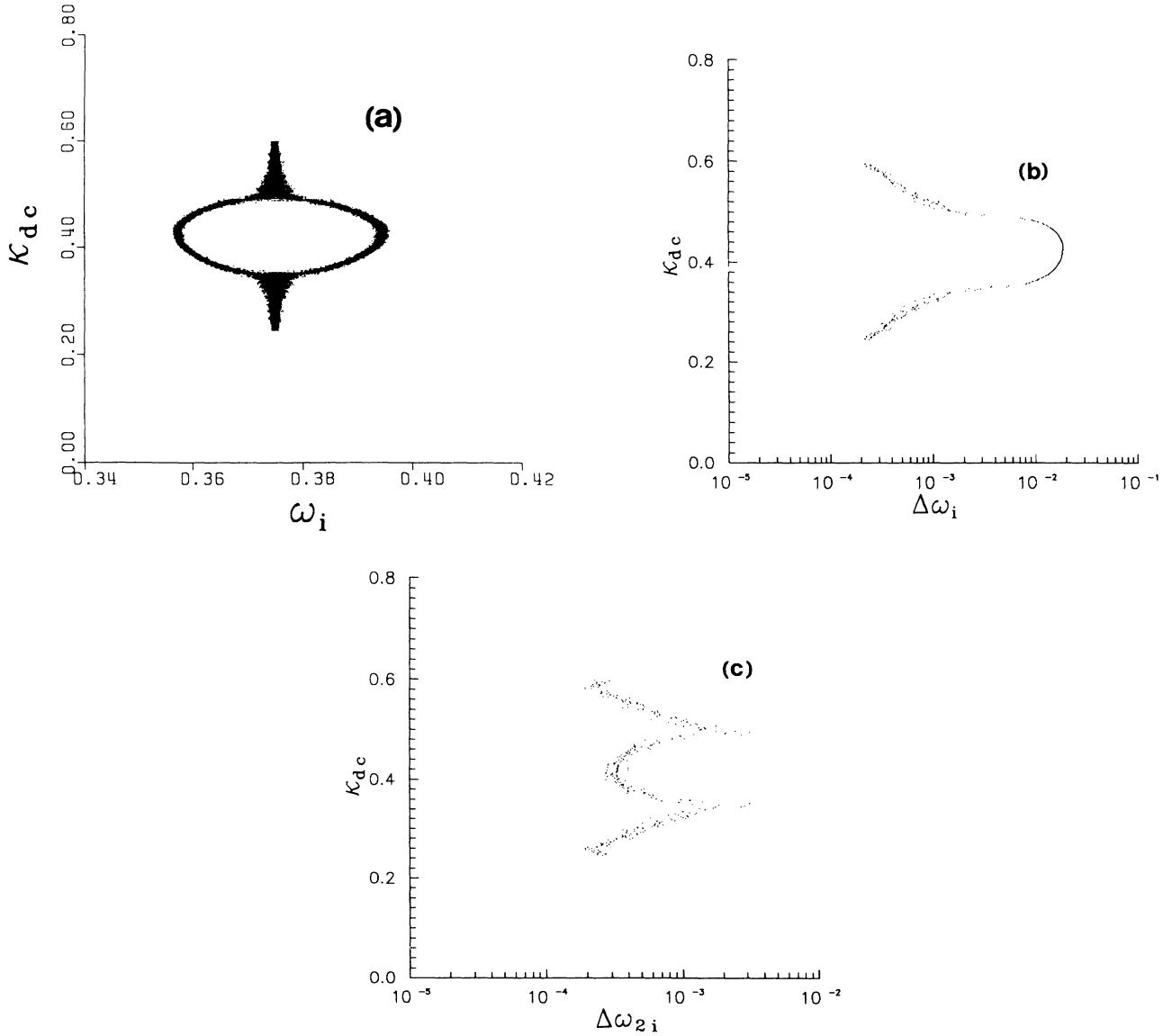

FIG. 5. Results of the stochastic map for the parameters of Fig. 1(c) and for Gaussian noise amplitudes of $\delta_T=0.01$ and $\delta_U=0$. (a) Measurements of the frequencies $\omega_i=2\pi/T_i$. (b) The standard deviation $\Delta\omega_i$ of the measurements in (a). (c) The standard deviation $\Delta\omega_{2i}$ obtained from every second measurement of ω_i.

dicted the increase to begin, not at the edge but at the value of the bias current for which the two eigenvalues break up on the real axis. This difference is due to the fact that the analysis was made for the one-dimensional map of the leading eigenvalue, and not for any specific direction in the two-dimensional map. In Fig. 3(a) we show the ensemble of measurements frequency for the case of $\kappa_{ac}=0.18$. Here we see, as was observed in Ref. 4, that a period doubling bifurcation has taken place. We did not observe any shift of the bifurcation points due to the thermal noise. Again, we find in accordance with Eq. (33) that the noise level rises as the bias approaches the bifurcation points. This is shown in Fig. 3(b), which is the counterpart to Fig. 2(b). Note that the extremely large standard deviation seen in Fig. 3(b) in the bifurcated region is not due to the thermal noise, but is merely an artifact of the two different characteristic frequencies. In order to overcome this artifact, we have in Fig. 3(c) shown the standard deviation of every second frequency measurement. Here the noise singularities corresponding to the bifurcation points are visible as two noise peaks. A similar plot is obtained when the other half of the frequency measurements are considered (the other branch of the bifurcated state).

Using the stochastic map approach, we can treat the noise in a simple manner, since we already know that we are concerned with a phase-locked step at the frequency of $\langle \omega_i \rangle = 2\omega_{ac}/m = 0.375$. From this, and the other fixed parameters of the system, we calculate the predicted standard deviation of the two variables. The noise used in these experiments was generated as a uniformly distributed ensemble with the noise amplitude δ ($\pm\delta/2$) again followed by a transformation into a Gaussian distribution. From Eq. (29) we then get the noise amplitude δ_T

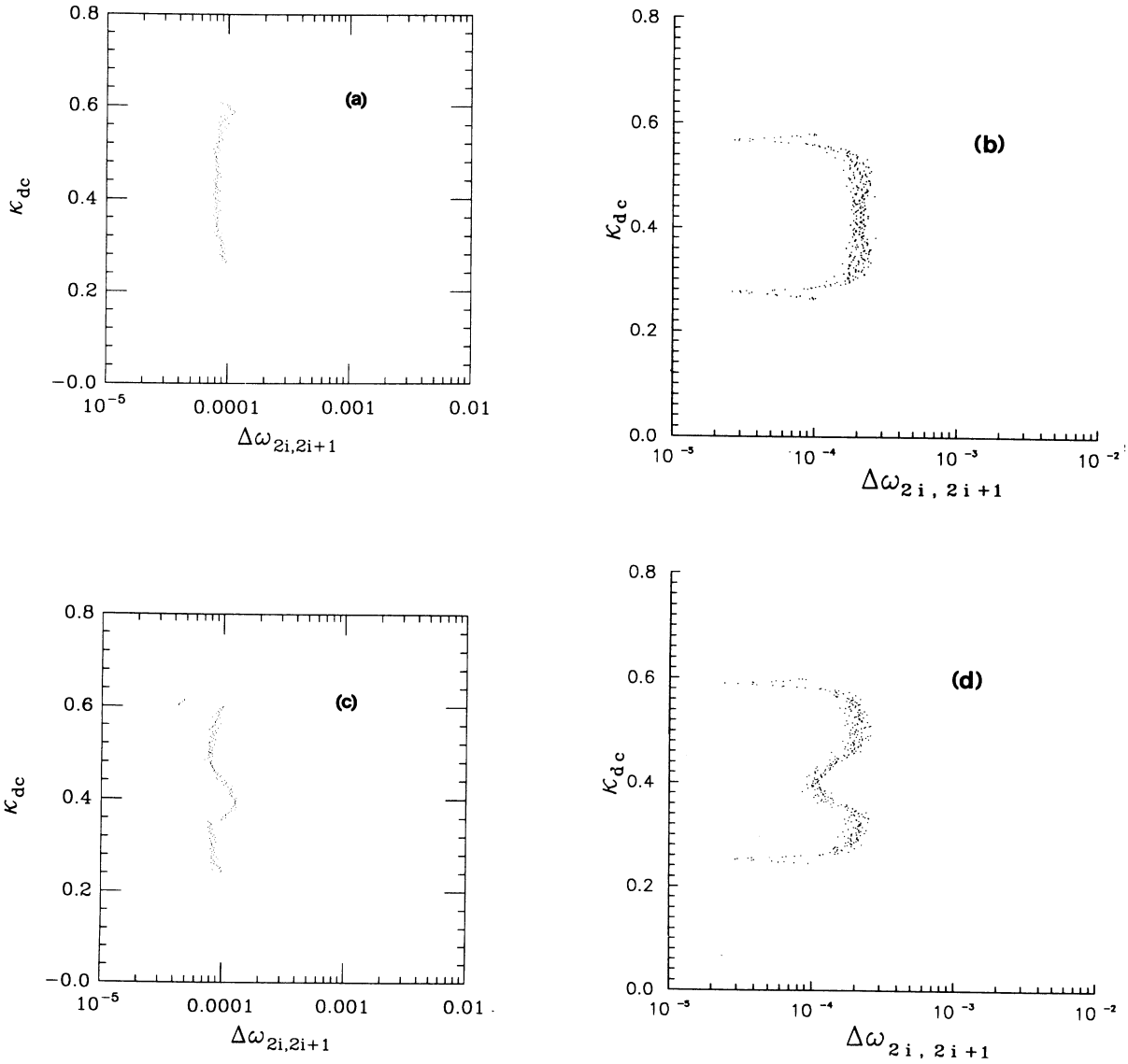

FIG. 6. Measurements made over two time of flights ($2T_k$) for the system parameters in Figs. 2–5. (a) $\kappa_{ac}=0.16$ for the stochastic ODE. (b) $\kappa_{ac}=0.16$ for the stochastic map. (c) $\kappa_{ac}=0.18$ for the stochastic ODE. (d) $\kappa_{ac}=0.18$ for the stochastic map.

for the time of flight to be $\delta_T \approx 0.0115$. The corresponding noise amplitude for the momentum dimension is similarly found to be $\delta_U \approx 0.001\,40$—i.e., the noise term of the momentum is a factor of 100 (in variance) less than the noise term for the time of flight. We therefore proceed, using the amplitudes $\delta_T = 0.01$ and $\delta_U = 0$. Figures 4 and 5 are the map counterparts to Figs. 2 and 3 for the ODE treatment. As seen from the plots, the results are almost identical to the ones obtained by the Langevin ODE treatment. We conclude that it is possible to construct a stochastic map describing the thermal noise influence on the LJJ. The thermal noise enters mainly through the time dimension of the map. We also believe that the final results are not critically dependent on the actual distribution of the stochastic processes, but of course on the chosen amplitude (temperature).

The measurements of the frequency made on the system above, were performed at the specific frequency of the soliton propagation. If we instead look at the frequency measurement made over two soliton periods (half the frequency) we do not expect to find any noise rise near an instability as seen from Eq. (35). This typical behavior is shown in Fig. 6 for the cases of both bias values and models. It is important to note that this is a general behavior of the noise properties near a period doubling bifurcation. As shown in Ref. 17 the squeezing of thermal noise in classical systems is found exactly in the parameter region, where fixpoints split up on the negative real axis, causing a stretch of the phase space in a specific direction (λ_1) and a squeezing in a perpendicular direction (λ_2) giving rise to the squeezed state.

IV. CONCLUDING REMARKS

We have investigated the noise properties of phase-locked fluxon motion in the simple framework of the particle model, in which the fluxon has no spatial extension, but is represented as a collective coordinate of relativistic nature. Analytic expressions were developed for the noise amplitudes to be used when a two-dimensional map approach is applied to study the dynamics of the fluxon motion and it was shown, by comparison to the more complete model of a stochastic ordinary differential equation, that the calculated noise amplitudes are in fact usable and the results of the two models were the same in the overall characteristics. Further, it was demonstrated that near an instability (period doubling bifurcation) the noise level increases dramatically in a specific direction of the phase space if the measurements are made at the frequency corresponding to the time of flight of the fluxon. This is in close correspondence to the squeezed noise states in classical systems, where a certain measurement done at a specific frequency in a specific direction in the phase space can result in a reduced noise level of the measured variable. It was shown, from a simple analytical treatment of the diagonalized map and from numerical experiments made on the two models, that the enhanced noise level near instabilities disappeared when the measurements were made at half the frequency of the fluxon motion.

---

*Present address: Department of Applied Physics, Stanford University, Stanford, California 94305.

[1]J.-J. Chang, Phys. Rev. B **34**, 6137 (1986).

[2]M. Salerno, M. R. Samuelsen, G. Filatrella, S. Pagano, and R. D. Parmentier, Phys. Lett. A **137**, 75 (1989).

[3]M. Salerno, M. R. Samuelsen, G. Filatrella, S. Pagano, and R. D. Parmentier, Phys. Rev. B **41**, 6641 (1990).

[4]M. Salerno, Phys. Lett. A **144**, 453 (1990).

[5]M. Salerno and M. R. Samuelsen, Phys. Lett. A **156**, 293 (1991).

[6]D. W. McLaughlin and A. C. Scott, Phys. Rev. A **18**, 1652 (1978).

[7]E. Jørgensen, V. P. Koshelets, R. Monaco, J. Mygind, M. R. Samuelsen, and M. Salerno, Phys. Rev. Lett. **45**, 1093 (1982).

[8]M. Salerno, E. Jørgensen, and M. R. Samuelsen, Phys. Rev. B **30**, 2635 (1984).

[9]M. Salerno, M. R. Samuelsen, and H. Svensmark, Phys. Rev. B **38**, 593 (1988).

[10]See, e.g., A. Barone and G. Paterno, *Physics and Applications of the Josephson Effect* (Wiley, New York, 1982).

[11]See, e.g., D. W. Jordan and P. Smith, *Nonlinear Ordinary Differential Equations* (Oxford University Press, New York, 1977).

[12]See, e.g., A. Papoulis, *Probability, Random Variables, and Stochastic Processes* (McGraw-Hill, New York, 1965).

[13]H. Svensmark and M. R. Samuelsen, Phys. Rev. A **36**, 2413 (1987).

[14]E. Helfand, Bell Syst. Tech. J. **58**, 2280 (1979).

[15]H. S. Greenside and E. Helfand, Bell Syst. Tech. J. **60**, 1927 (1981).

[16]See, e.g., W. H. Press, B. P. Flannery, S. A. Teukolsky, and W. T. Vetterling, *Numerical Recipes* (Cambridge University Press, Cambridge, England, 1986).

[17]H. Svensmark, Phys. Rev. A **45**, 1924 (1992).